





Hyperglycaemia, pregnancy outcomes and maternal metabolic disease risk during pregnancy and lactation in a lean gestational diabetes mouse model

Angela J. C. Tol¹, Kaja Hribar¹, Janine Kruit¹ , Laura Bongiovanni^{2,3}, Marcel A. Vieira-Lara¹, Mirjam H. Koster¹ , Niels J. Kloosterhuis¹, Rick Havinga¹, Martijn Koehorst⁴, Alain de Bruin^{1,2}, Barbara M. Bakker¹ , Maaïke H. Oosterveer^{1,4} and Eline M. van der Beek¹ 

¹Department of Pediatrics, University of Groningen, University Medical Center Groningen, Groningen, the Netherlands

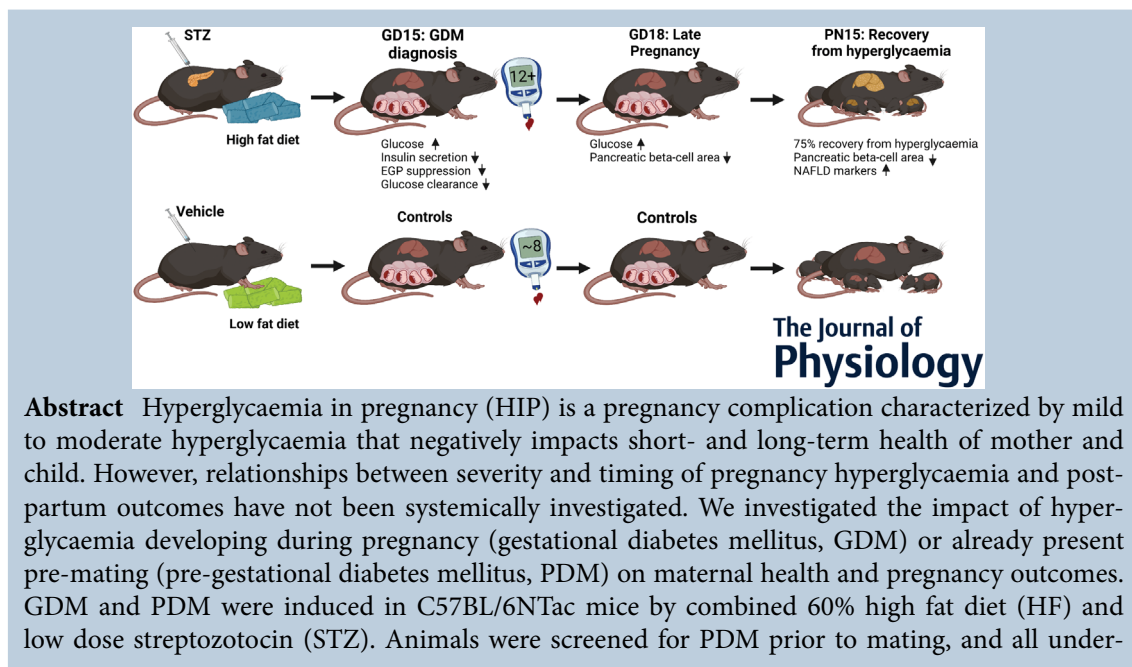
²Department of Biomolecular Health Sciences, Faculty of Veterinary Medicine, Utrecht University, Utrecht, the Netherlands

³Faculty of Veterinary Medicine, University of Teramo, Teramo, Italy

⁴Department of Laboratory Medicine, University Medical Center Groningen, Groningen, the Netherlands

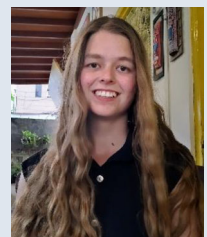
Handling Editors: Laura Bennet & Christopher Lear

The peer review history is available in the Supporting Information section of this article (<https://doi.org/10.1113/JP284061#support-information-section>).



Abstract Hyperglycaemia in pregnancy (HIP) is a pregnancy complication characterized by mild to moderate hyperglycaemia that negatively impacts short- and long-term health of mother and child. However, relationships between severity and timing of pregnancy hyperglycaemia and post-partum outcomes have not been systemically investigated. We investigated the impact of hyperglycaemia developing during pregnancy (gestational diabetes mellitus, GDM) or already present pre-mating (pre-gestational diabetes mellitus, PDM) on maternal health and pregnancy outcomes. GDM and PDM were induced in C57BL/6NTac mice by combined 60% high fat diet (HF) and low dose streptozotocin (STZ). Animals were screened for PDM prior to mating, and all under-

Angela Tol is a PhD candidate at the University Medical Center in Groningen. She is interested in the effects of adverse pregnancy conditions, and in particular the effects of maternal diabetes, on offspring health and development. She investigated the effects of maternal diabetes on maternal, fetal and placental pathophysiology using a preclinical model for gestational diabetes.



M. H. Oosterveer and E. M. van der Beek contributed equally to this work.

went an oral glucose tolerance test on gestational day (GD)15. Tissues were collected at GD18 or at postnatal day (PN)15. Among HFSTZ-treated dams, 34% developed PDM and 66% developed GDM, characterized by impaired glucose-induced insulin release and inadequate suppression of endogenous glucose production. No increased adiposity or overt insulin resistance was observed. Furthermore, markers of non-alcoholic fatty liver disease (NAFLD) were significantly increased in PDM at GD18 and were positively correlated with basal glucose levels at GD18 in GDM dams. By PN15, NAFLD markers were also increased in GDM dams. Only PDM affected pregnancy outcomes such as litter size. Our findings indicate that GDM and PDM, resulting in disturbances of maternal glucose homeostasis, increase the risk of postpartum NAFLD development, related to the onset and severity of pregnancy hyperglycaemia. These findings signal a need for earlier monitoring of maternal glycaemia and more rigorous follow-up of maternal health after GDM and PDM pregnancy in humans.

(Received 3 November 2022; accepted after revision 10 March 2023; first published online 3 April 2023)

Corresponding author E. M. van der Beek: Department of Pediatrics, University Medical Center Groningen, Hanzeplein 1, Postbus 30 001, Groningen, 9700 RB, the Netherlands. Email: e.m.van.der.beek@umcg.nl

Abstract figure legend Streptozotocin and high fat diet were used to induce gestational diabetes mellitus (GDM) in female BL6/NTac mice. Pregnant dams underwent an oral glucose tolerance test at gestational day (GD)15 to confirm GDM diagnosis. By GD18, dams were hyperglycaemic and showed a reduction in pancreatic β -cells. By postnatal day (PN)15, dams additionally had developed an increase in non-alcoholic fatty liver disease (NAFLD) markers, despite the majority of the dams having recovered from hyperglycaemia.

Key points

- We studied the impact of high-fat diet/streptozotocin induced hyperglycaemia in pregnancy in mice and found that this impaired glucose tolerance and insulin release.
- Litter size and embryo survival were compromised by pre-gestational, but not by gestational, diabetes.
- Despite postpartum recovery from hyperglycaemia in a majority of dams, liver disease markers were further elevated by postnatal day 15.
- Maternal liver disease markers were associated with the severity of hyperglycaemia at gestational day 18.
- The association between hyperglycaemic exposure and non-alcoholic fatty liver disease signals a need for more rigorous monitoring and follow-up of maternal glycaemia and health in diabetic pregnancy in humans.

Introduction

An estimated 17% of live births worldwide are currently affected by hyperglycaemia in pregnancy (HIP), of which 80% is due to gestational diabetes mellitus (GDM) and 20% to pre-existing diabetes, either known (pre-gestational diabetes mellitus, PDM) or first detected during pregnancy (diabetes in pregnancy) (International Diabetes Federation, 2021). The global rise in obesity and unhealthy lifestyles predicts that HIP incidence will rise further (Ferrara, 2007; International Diabetes Federation, 2019; Kim et al., 2010). HIP is associated with adverse perinatal outcomes and compromised long-term metabolic health of both mother and child

(Farahvar et al., 2019; Kampmann, 2015; Zisser et al., 2010).

GDM, defined as glucose intolerance with first onset during pregnancy, is clinically diagnosed using an oral glucose tolerance test (OGTT) between 24 and 28 weeks of pregnancy. GDM can result from reduced insulin sensitivity, inadequate insulin secretion, or a combination of both (Powe et al., 2016). Reduced insulin sensitivity is common in overweight GDM patients and results in fasting hyperinsulinaemia and enhanced postprandial insulin secretion (Powe et al., 2016). Inadequate insulin secretion is more common in lean GDM patients resulting in reduced fasting and postprandial insulin levels (Catalano, 2014; Cheney et al., 1985, p.31;

Liu et al., 2018). After delivery, women with former GDM are at an increased risk for metabolic complications such as type 2 diabetes and non-alcoholic fatty liver disease (NAFLD) (Ajmera et al., 2016; Chen et al., 2021; Forbes et al., 2011; Lavrentaki et al., 2019). It has been suggested that the severity of hyperglycaemia, defined as glucose levels and time of onset, is related to maternal and pregnancy outcomes (The HAPO Study Cooperative Research Group, 2008), but this has not been systemically investigated. Insights in the relation between severity of hyperglycaemia and maternal outcomes would allow for better clinical care, increased quality of life and reduced morbidity.

Preclinical studies are key to generating in-depth knowledge on GDM pathophysiology, and they serve as a base to define interventions that mitigate disease risk. Animal models for GDM are generally developed targeting either insulin sensitivity or insulin secretion (Lilao-Garzón et al., 2020; Pasek & Gannon, 2013). Most models develop (severe) hyperglycaemia prior to pregnancy (Pasek & Gannon, 2013), limiting the ability to link the severity of hyperglycaemia to adverse health consequences and possible translation to the human situation. Recently, a mouse model for lean GDM was developed combining short term high fat (HF) feeding and multiple low-dose streptozotocin (STZ) injections (Li et al., 2020). This two-hit approach (HFSTZ), which was designed to concomitantly impair insulin sensitivity and secretion, resulted in transient gestational hyperglycaemia and glucose intolerance without increased body weight or adiposity. Most dams who developed GDM recovered from hyperglycaemia after delivery (Li et al., 2020). The initial characterization of this mouse model allows for further investigation of the link between severity of hyperglycaemia and adverse outcomes in mothers and their offspring.

The current study aimed to assess the impact of hyperglycaemia and its severity on maternal glucose homeostasis, adiposity, pregnancy outcomes and NAFLD susceptibility during pregnancy and lactation in this mouse model for lean gestational hyperglycaemia. We hypothesized that hyperglycaemia induced by HFSTZ treatment is driven by a combination of insulin resistance and defective insulin secretion and that more severe and/or earlier onset would result in worsened postpartum recovery from hyperglycaemia, NAFLD susceptibility and pregnancy outcomes.

Methods

Ethical approval

Animal procedures were performed in compliance with EU legislation (Directive 2010/63/EU). The study protocol was approved by the Dutch Central Committee Animal

Testing (no. AVD1050020185445) and the Institutional Animal Care and Use Committee of the University of Groningen. All institutional and national guidelines for the care and use of laboratory animals were followed.

Animals

In total, 181 9-week-old, nulliparous C57Bl/6NTac females (Table 1), and 55 8-week-old C57Bl/6NTac males were purchased (Taconic Biosciences, Denmark, Albany, NY, USA). Mice were housed in individually ventilated cages under a 12 h light–dark cycle (07.00–19.00 h). Females were pair-housed and fed 10E% low fat (LF; D12450Ji, Research Diets, Wijk bij Duurstede, Netherlands), or 60E% HF diet (D12492i, Research Diets, Table 2) immediately upon arrival. Males were housed individually and fed chow (RMH-B, AB-diets, Woerden, Netherlands). Both food and drinking water were provided ad libitum. Body weight (BW) was monitored weekly. Experimenters were not blinded, except for the pathologist performing histopathological analysis.

Experimental set-up

Upon arrival, females were assigned to one of four groups using a computer-generated sequence (Research Randomizer, randomizer.org). The treatment groups were: LF+vehicle (LF), LF+STZ (LFSTZ), HF+vehicle (HF) and HF+STZ (HFSTZ). After 4 weeks on the assigned diets, mice received either 60 mg/kg STZ (S0130, Sigma-Aldrich, Darmstadt, Germany) or vehicle intraperitoneally for three consecutive days as described previously (Li et al., 2020). Maternal GDM and PDM development were studied using gestational day (GD)18 (pregnancy cohort) and postnatal day (PN)15 (lactation cohort) end points representing late pregnancy and lactation (Fig. 1). In the lactation cohort, pups were born on GD19.5 and litter sizes were standardized to four to six pups with at least two male and two female pups at PN2 whenever possible. A total of five litters were composed of one sex only, as no pups of the other sex were available for cross-fostering. The LFSTZ group was not included in the lactation cohort as LFSTZ-treated dams did not display gestation-specific hyperglycaemia in current (Fig. 2) and previous studies (Li et al., 2020).

Sample size calculation

Sample size was calculated with G*Power (<http://www.gpower.hhu.de/>), using $\beta = 0.9$, $\alpha = 0.05$, effect size = 1.67 (mean difference = 5, SD = 3), and identical group sizes. The effect size was based on the previously observed difference in blood glucose between GDM and LF dams

Table 1. Number of female breeders, number of pregnant mice, lost litters, exclusions, and final number of included animals

	Breeders	Pregnant (%)	Lost litters (%)	Excluded	Reason exclusion	Included till GD18	
Pregnancy time point (GD18)							
Total	70	40 (57)	NA	7		35	NA
LF	12	7 (58)		1	Litter <2	6	
LFSTZ	19	12 (63)		4	2 × litter <2 1 × severe PDM* 1 × premature [†]	8	
HF	12	7 (58)		1	Litter <2	6	
GDM	20	9 (45)		1	Non-responder	8	
PDM	7	5 (71)		NA		5	
Lactation time point (PN15)							
						Included till PN2	Included till PN15
Total	111	72 (65)	11 (15)	1		61	35
LF	15	11 (73)	1 (9)	NA		10	10
HF	28	19 (68)	2 (11)	NA		17	9
GDM	45	28 (62)	5 (18)	1	Non-responder	23	12
PDM	23	14 (61)	3 (21)	NA		11	4

Lost litter refers to death of all pups and/or cannibalization between birth and PN2. *Dam developed severe PDM and humane end point was applied as random blood glucose values exceeded 30 mmol/l by mid-gestation. [†]Timing of pregnancy was misdiagnosed; litter was terminated at GD13.5 instead of GD17.5. Non-responders were defined as HFSTZ treated dams with 2 h blood glucose <12 mmol/l during the OGTT. The HFSTZ group is depicted as GDM and PDM, depending on their hyperglycaemic phenotype as described in Fig. 1. DM, diabetes mellitus; GD, gestational day; GDM, gestational diabetes mellitus; HF, high fat diet; HFSTZ, high fat diet + streptozotocin; LF, low fat diet; LFSTZ, low fat diet + streptozotocin; NA, not applicable; PDM, pre-gestational diabetes mellitus; PN, postnatal day.

Table 2. Composition of diets

	LF (D12450Ji)	HF (D12492i)
Carbohydrate (kcal %)	70	20
Protein (kcal %)	20	20
Fat (kcal %)	10	60
Energy density (kcal/g)	3.82	5.21

Diet composition information was obtained from Research Diets product data sheets. For further details:

LF: <https://researchdiets.com/formulas/d12450J>; HF: <https://researchdiets.com/formulas/d12492>.

at 20 min (peak glucose in LF control dams) during the OGTT (Li et al., 2020). This resulted in a group size of 9. Due to expected dropout related to development of PDM, pregnancy rate and lost litters, final animal numbers are different (Table 1). Additionally, in the lactation cohort, about half the dams of the HF and HFSTZ groups were switched to LF at PN2 to assess the contribution of HF during lactation, resulting in double the number of breeders (Table 1). As the postnatal diet effect is beyond the scope of the current study, data from the dams that were switched to LF are included until PN2 only. Within

the HFSTZ group, the study was powered to have sufficient animals in the GDM group, leaving the PDM group underpowered.

The number of breeding males required was determined assuming that each day, maximally 1 in 3 dams would be in pro-oestrus. Reusing males between sub-cohorts resulted in a total number of 55 male breeders.

Breeding

Twelve days after STZ/vehicle injections, vaginal smears were taken daily to assess the oestrous cycle. Dams in pro-oestrus were bred 1:1 by adding a randomly chosen male breeder to the female cage for 16 h overnight, after which females were housed individually with cage locations randomized. A vaginal plug the next morning was considered as GD1. When no plug appeared, oestrous cycle assessment and pro-oestrus breeding (with a different male) continued for a maximum of three matings within a 10-day period. Thirty eight percent (69/181) of the dams did not become pregnant (Table 1) and were excluded except for RBG and OGTT

testing; see section ‘Hyperglycaemia and glucose tolerance in non-pregnant dams’.

Hyperglycaemia detection and diabetes diagnosis

To monitor glycaemic changes indicating diabetes development, random blood glucose (RBG) levels under non-fasted conditions were analysed in blood samples collected from a tail cut using an Accu-Chek Performa glucose meter (Roche, Mannheim, Germany). RBG was measured in a random order between 09.00 and 10.00 h prior to STZ injection, at GD0/GD7/GD14/GD18, and PN8/PN15.

Based on phenotype, HFSTZ-treated dams were subdivided into a PDM and a GDM group (Fig. 1). HFSTZ mice that developed hyperglycaemia prior to pregnancy (defined as RBG > 12 mmol/l at GD0; Li et al., 2020) were classified as PDM and analysed separately. Dams with RBG < 12 mmol/l at GD0 were classified as normoglycaemic and screened for GDM at GD15 (see section OGTT). PN15 RBG levels were used to assess recovery, defined as RBG < 12 mmol/l.

Hyperglycaemia and glucose tolerance in non-pregnant dams

To assess if hyperglycaemia development was specific to gestation, a group of non-pregnant HFSTZ dams ($n = 20$) were subjected to RBG measurements at similar time intervals as their pregnant counterparts (7, 14 and 18 days after the last unsuccessful mating). In addition, a random

selection of non-pregnant animals underwent an OGTT 15 days after the last unsuccessful mating.

OGTT

At GD15, roughly corresponding to the moment of clinical GDM diagnosis in human pregnancy, females were fasted for 6 h (06.00–12.00 h) in their home cage followed by fasting blood glucose measurement using an Accu-Chek Performa glucose meter (Roche, Mannheim, Germany) and collection of a small blood sample from the tail on filter paper (Satorius Stedim, TFN 180 g/m² Zug, Switzerland). Glucose tolerance was subsequently assessed by OGTT. Stably labelled glucose was included in the OGTT to enable dissection of endogenous glucose production (EGP), and to determine insulin sensitivity using mathematical modelling of tracer-based glucose kinetics (van Dijk et al., 2013; Vieira-Lara et al., 2023). D-Glucose (1 g/kg BW in a 200 g/l solution, of which 5% w/w stable isotope-labelled [6,6-²H₂]glucose tracer (Cambridge Isotope Laboratories, Andover, MA, USA), was administered by oral gavage. Glucose administration was conducted in a random order. Blood glucose measurement and blood spots for tracer analysis were taken at eight time points. Additionally, blood spots to quantify insulin levels were taken at six time points.

HFSTZ-treated dams that were normoglycaemic at GD0 were diagnosed with GDM if the 2 h OGTT blood glucose was >12 mmol/l. Two HFSTZ-treated dams with 2 h blood glucose <12 mmol/l were considered non-responders and excluded (Table 1).

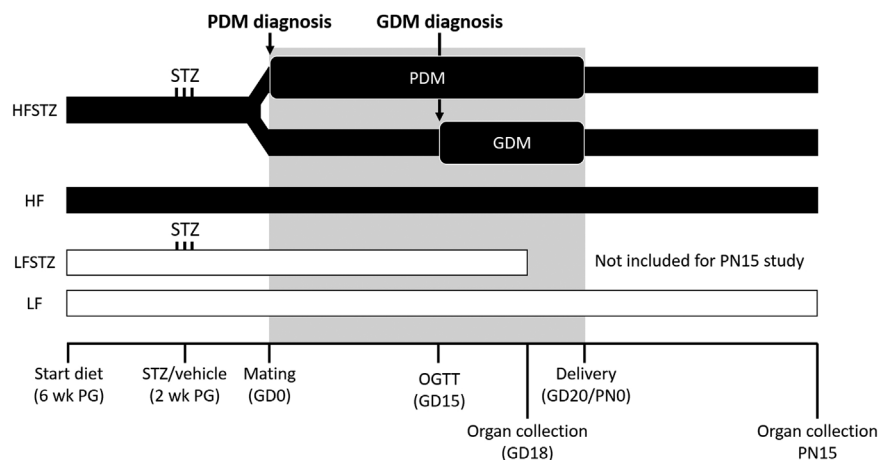


Figure 1. Schematic overview of the experimental design, including both the GD18 and PN15 end points Mice were fed HF or LF diet starting 6 weeks prior to gestation (PG). After 4 weeks of diet, mice were administered STZ or vehicle i.p. for three consecutive days. Random blood glucose (RBG) was measured on the day of mating to discriminate between HFSTZ dams that had developed PDM versus HFSTZ dams that had remained normoglycaemic. On GD15, GDM was confirmed using an OGTT. Dams in the pregnancy cohort were terminated on GD18. For the PN15 (lactation) cohort, litter size was determined and standardized on PN2. Postpartum recovery was evaluated by a random blood glucose measure on PN15, which was also the time point of termination.

Organ collection

Dams were terminated in a random order by cardiac puncture after being fully anaesthetized in a closed chamber with a steady flow of isoflurane at GD18. For PM15 dams, subcutaneous administration of 75 mg/kg body weight of ketamine and 1 mg/kg dexmedetomidine was used. Tissues were excised and snap-frozen or fixed in 4% (w/v) formaldehyde in PBS. PN15 dams received oxytocin (1IU, Synthocinon®, Sigma-Tau Industrie Pharmaceutische Riunite, Darmstadt, Germany) and were milked for up to 20 min prior to termination. The milk analysis is, however, beyond the scope of this study. GD18 litters were collected by removing the whole uterus and separating fetuses and placentas on ice. Number of fetuses and resorptions (Joachim et al., 2003) were counted.

Insulin levels and HOMA-IR

Blood samples for insulin measurement were collected on filter paper by tail bleeding for random insulin determination at GD0, GD18, PN15, and during the OGTT. Insulin measurements were performed by ELISA (Crystal Chem cat. no. 90010 and 90020, Zaandam, Netherlands), as described previously (Martin et al., 2012). In brief, 6 mm discs were punched from the blood spots and insulin was extracted by adding the spots into the assay wells in 95 μ l diluent. Insulin levels on the day of termination (GD18/PN15) were quantified by ELISA (Crystal Chem) using 5 μ l of plasma. To correct for differences in sample volumes between blood spots and plasma samples, the concentrations derived from the blood spots were multiplied by 1.28, which is based on a series of measurements comparing blood spots and matching plasma samples (Dommerholt et al., 2020). Homeostatic model assessment for insulin resistance (HOMA-IR) was calculated as previously described (van Dijk et al., 2013).

Estimation of EGP rates, glucose clearance rates, and insulin sensitivity

Fractional distribution of [6,6-²H₂]glucose was determined by gas chromatography–quadrupole mass spectrometry (Agilent 9575C Inert MSD, Agilent Technologies, Santa Clara, CA, USA), as described previously (van Dijk et al., 2013). Glucose was extracted from the dried bloodspots and converted to its pentaacetate derivative. Positive chemical ionization with ammonia enabled monitoring of ions' *m/z* 408–412 (corresponding to m0–m4 mass isotopologues), which were corrected for the fractional distribution due to natural abundance of isotopes by multiple linear regression (Lee et al., 1991). The m2 value represents the fractional contribution of

the administered tracer and was used in the calculations of blood glucose kinetics.

Kinetic parameters, endogenous glucose production (EGP) and indices for insulin sensitivity were computed according to Vieira-Lara et al. (2023). In brief, the compartment model depicted in Fig. 2 was used, with a gastrointestinal compartment (GI tract, compartment 1) and a blood plasma compartment (compartment 2). Here labelled glucose pools (tracer) are represented by q_1 and q_2 , and unlabelled glucose by Q_1 and Q_2 . The bioavailability of the tracer is given by: $F = k_1/(k_1 + k_L)$

Plasma insulin levels were fitted to: $INS(t) = C \times (e^{-k_e t} - e^{-k_a t})$

Average insulin over a specific time range ($INS_{t_1 \rightarrow t_2}$) was computed as: $INS_{t_1 \rightarrow t_2} = \frac{AUC_{t_1 \rightarrow t_2}}{t_2 - t_1}$ in which $AUC_{t_1 \rightarrow t_2}$ is the area under the fitted insulin curve from t_1 to t_2 . The time-averaged EGP was computed analogously, based on the area under the EGP time course.

The peripheral insulin sensitivity (IS-P) was defined as: $IS-P_T = \frac{k_2}{INS_{0 \rightarrow 120}}$

The liver insulin sensitivity (IS-L) was defined as: $IS-L_T = \frac{1000}{EGP_{t_1 \rightarrow t_2} \times INS_{t_1 \rightarrow t_2}}$ as described previously in (Matsuda & DeFronzo, 1999).

All calculations were conducted in Python using Jupyter Notebook (v5.7.4).

Pancreas analysis

Formalin-fixed pancreatic tissues were embedded in paraffin, sectioned, deparaffinized and rehydrated using standard techniques. Two pancreas samples (1 \times GD18 GDM, 1 \times PN15 PDM) were lost during collection and therefore missing in this analysis. For β -cell area measurements, pancreatic tissue was stained for insulin using immunocytochemistry. Pancreases

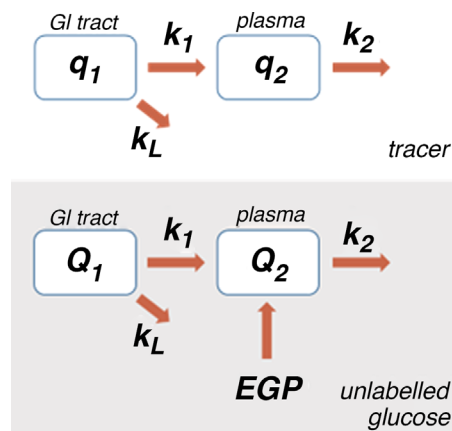


Figure 2. Proposed compartment model for tracer and unlabelled glucose

[Colour figure can be viewed at wileyonlinelibrary.com]

were sectioned transversely (dorsal to ventral) and eight 7 μm sections were collected at 100 μm intervals. The eight sections per pancreas were randomized between staining batches to ensure equal distribution of groups and animals between batches. Sections were stained with guinea pig anti-insulin primary antibody (7.4 mg/l, cat. no. A0564, Dako, Glostrup, Denmark), rabbit anti-guinea pig IgG H&L secondary antibody (5 mg/l, cat. no. Ab102360, Abcam, Cambridge, UK), and goat anti-rabbit immunoglobulins/horseradish peroxidase tertiary antibody (1.25 mg/l, cat. no. P0448, Dako, Glostrup, Denmark), followed by DAB peroxidase substrate kit (Substrate Kit-4100, Vector Laboratories Inc., Newark, CA, USA), and Mayer's haematoxylin staining (cat. no. MHS32-1L, Sigma-Aldrich, Merck). Slides were scanned using a Hamamatsu NanoZoomer (Hamamatsu Photonics, Hamamatsu, Japan). The insulin-positive and total area of each section were determined using semi-quantitative analysis with colour deconvolution and threshold selection of positive stained area using ImageJ Fiji Software (Schindelin et al., 2012). The insulin-positive area was calculated by dividing the sum of the insulin-positive stained area of all sections by the total sum of the tissue area of all sections. For immunofluorescence, sections were incubated overnight at 4°C with antibodies against insulin (1:1000, cat. no. A0564, Dako, Glostrup, Denmark) and glucagon (1:250, cat. no. A0565, Dako, Glostrup, Denmark), followed by secondary antibodies (1:250, cat. no. A11011, A11073, Thermo Fisher Scientific, Waltham MA, USA) and 4',6-diamidino-2-phenylindole (DAPI) (Roche, Mannheim, Germany). Immunofluorescence staining was quantified using ImageJ by a blinded researcher.

Liver and plasma analysis

Histopathological scoring for NAFLD markers, apoptotic and mitotic figures on haematoxylin and eosin (H&E)-stained liver sections was performed blinded by a board-certified veterinary pathologist as described previously (Hübscher, 2006; Kleiner et al., 2005). The pathologist checked several slides per sample after which one representative slide was selected for the detailed analysis. One histological PDM liver sample was lost during collection and is therefore missing in this analysis. Hepatic lipid levels (triglycerides (TGs), cat. no. 11877771216, Roche Diagnostics; cholesterol, total: cat. no. 11491458-216, Roche Diagnostics; free: cat. no. 41035, Spinreact, Girona, Spain) were determined biochemically using commercially available kits. Esterified cholesterol was calculated by subtracting free cholesterol values from total cholesterol values. Plasma TGs and non-esterified fatty acids were measured using the same kits (Roche Diagnostics). Hepatic glycogen was determined as previously described (Bergmeyer, 1974). Plasma leptin levels

were analysed using a Mouse Leptin ELISA kit (cat. no. 90030, Crystal Chem) according to the manufacturer's protocol. Plasma alanine aminotransferase (ALT) was analysed using a Cobas 6000 analyser with standard reagents using 50 μl of plasma (Roche Diagnostics).

Statistics

Data are presented as means \pm SD with the dam or litter as experimental unit, and therefore 'n' represents the number of dams or, for the pregnancy outcomes, the number of litters. Normality was assessed and between-group differences were tested using one-way ANOVA followed by Tukey's multiple comparison test in case of normally distributed data, or the Kruskal–Wallis test followed by Dunn's multiple comparisons test in case of non-normally distributed data or inability to assess normality ($n < 10$). For time course graphs, mixed model analyses were followed by Bonferroni's correction. Correlations within the HFSTZ (GDM+PDM) and GDM group alone were assessed using Pearson's or Spearman's correlation coefficient. All statistical analyses were performed using GraphPad Prism 9 software (GraphPad Software Inc., San Diego, CA, USA). Two-sided $P < 0.05$ was considered statistically significant.

Results

HFSTZ treatment impairs glucose tolerance and insulin response during the first 30 min in pregnant mice

Based on GD0 RBG concentrations, 34% of HFSTZ-treated dams displayed hyperglycaemia (RBG > 12 mmol/l) pre-gestation and were classified as PDM (Table 1). The remaining 66% was normoglycaemic (RBG < 12 mmol/l) pre-gestation and developed hyperglycaemia during gestation.

GDM diagnosis was confirmed by OGTT on GD15 (Fig. 3). As GD15 OGTT results were comparable between pregnancy and lactation cohorts, results were combined for analysis. Fasting blood glucose prior to the OGTT was slightly, yet significantly, increased in GDM compared to LF/HF (Fig. 3A and Table 3). In PDM dams, fasting blood glucose values were considerably and significantly higher than in all other groups. Fasting blood insulin was comparable between groups ($P = 0.1248$, Fig. 3B and Table 3) and HOMA-IR was increased in PDM compared to HF dams only (Fig. 3C). Throughout the OGTT, blood glucose values in GDM and PDM were significantly higher compared to LF and HF dams (Fig. 3A and Table 3). The LFSTZ group demonstrated a modest impairment in glucose tolerance (Fig. 3D), while blood glucose levels of HF dams were only significantly increased after 20,

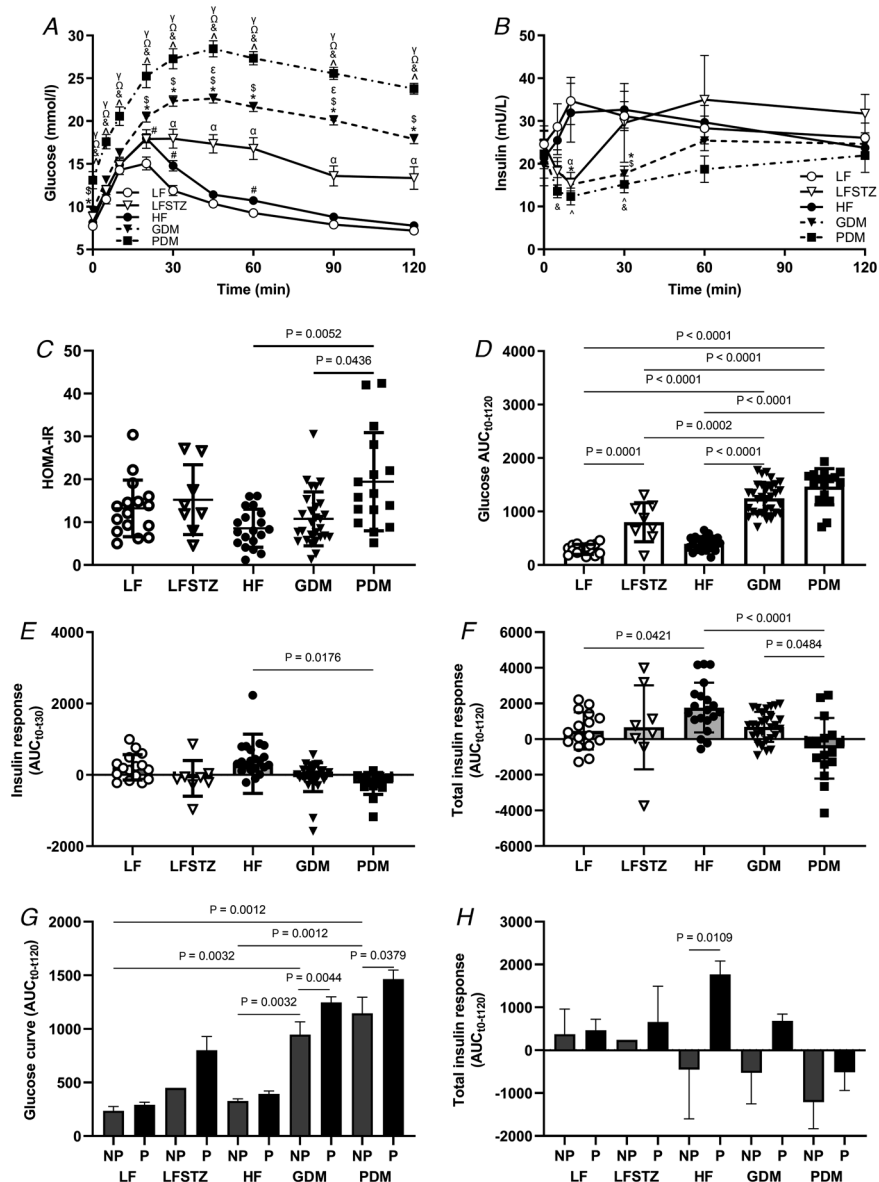


Figure 3. HFSTZ-induced lean GDM and PDM result in severe impairment of glucose tolerance and insulin release during the first 30 min and is further impaired by gestation

A, blood glucose concentrations (mmol/l) from tail blood throughout the OGTT at GD15, used to diagnose GDM development. **B**, blood insulin concentrations (mU/l) from tail blood throughout the OGTT at GD15. **C**, HOMA-IR calculated using GD15 fasted glucose and insulin concentrations as described previously van Dijk et al., 2013. **D**, glucose AUC, corrected for t_0 glucose. **E**, insulin AUC during the first 30 min of the OGTT, corrected for t_0 insulin. **F**, GD15 OGTT AUC of insulin from t_0 to t_{120} using t_0 insulin as a baseline. **G**, OGTT glucose clearance AUC, pregnant vs. non-pregnant comparison. **H**, OGTT insulin response AUC, pregnant vs. non-pregnant comparison. Data are means \pm SEM for readability (A and B) or means \pm SD (C–F). A and B: $n = 16$ (LF), 22 (HF), 8 (LFSTZ), 31 (GDM), 16 (PDM). G–H: $n = 4$ (LF-np), 16 (LF), 1 (LFSTZ-np), 8 (LFSTZ), 6 (HF-np), 22 (HF), 12 (GDM-np), 31 (GDM), 6 (PDM-np), 16 (PDM). Mixed model analysis followed by Bonferroni's correction (A and B) with absolute P -values for each comparison given in the Statistical Summary Document, one-way ANOVA followed by Tukey's multiple comparison test (D–F) or the Kruskal–Wallis test followed by Dunn's multiple comparison test (C, G, H). Statistical outliers (ROUT method, $Q = 1\%$), were removed prior to analysis for C ($n = 5$), E ($n = 1$) and F ($n = 5$). *GDM vs. LF, 3 GDM vs. HF, 5 PDM vs. LF, 7 PDM vs. HF, 9 LFSTZ vs. GDM, a LFSTZ vs. PDM, b LFSTZ vs. LF, c HF vs. LF. AUC, area under the curve; GD, gestational day; GDM, gestational diabetes mellitus; HF, high fat diet; L, lactation; LF, low fat diet; LFSTZ, low fat + streptozotocin; NP, non-pregnant; P, pregnant; PDM, pregestational diabetes mellitus; PN, postnatal day.

Table 3. P-values of OGTT glucose, OGTT insulin and random glucose time points

	LF vs. LFSTZ	LF vs. HF	LF vs. GDM	LF vs. PDM	LFSTZ vs. GDM	LFSTZ vs. PDM	HF vs. GDM	HF vs. PDM	GDM vs. PDM
Fig. 3A: OGTT glucose									
t ₀	>0.9999	>0.9999	0.0043	0.0008	>0.9999	0.0136	0.0088	0.0017	0.0362
t ₅	>0.9999	>0.9999	0.0210	<0.0001	>0.9999	0.0001	0.4292	<0.0001	0.0008
t ₁₀	>0.9999	>0.9999	0.0922	0.0003	>0.9999	0.0026	0.6817	0.0011	0.0175
t ₂₀	0.4916	0.0335	<0.0001	<0.0001	0.6016	0.0036	0.0269	0.0007	0.0401
t ₃₀	0.0051	0.0171	<0.0001	<0.0001	0.0472	0.0001	<0.0001	<0.0001	0.0106
t ₄₅	0.0015	0.5143	<0.0001	<0.0001	0.0099	<0.0001	<0.0001	<0.0001	0.0002
t ₆₀	0.0053	0.0004	<0.0001	<0.0001	0.0582	0.0001	<0.0001	<0.0001	<0.0001
t ₉₀	0.0151	0.3900	<0.0001	<0.0001	0.0048	<0.0001	<0.0001	<0.0001	<0.0001
t ₁₂₀	0.0212	0.7385	<0.0001	<0.0001	0.0981	0.0003	<0.0001	<0.0001	<0.0001
Fig. 3B: OGTT insulin									
t ₀	>0.9999	>0.9999	>0.9999	>0.9999	>0.9999	>0.9999	>0.9999	>0.9999	>0.9999
t ₅	>0.9999	>0.9999	0.9558	0.1501	>0.9999	>0.9999	0.8153	0.0277	0.3996
t ₁₀	0.0480	>0.9999	0.0319	0.0118	>0.9999	>0.9999	0.2586	0.1142	>0.9999
t ₃₀	>0.9999	>0.9999	0.0173	0.0043	>0.9999	>0.9999	0.0327	0.0094	>0.9999
t ₆₀	>0.9999	>0.9999	>0.9999	0.2996	>0.9999	>0.9999	>0.9999	0.3666	0.9632
t ₁₂₀	>0.9999	>0.9999	>0.9999	>0.9999	>0.9999	>0.9999	>0.9999	>0.9999	>0.9999
Fig. 5A: random glucose									
GD -14	>0.9999	>0.9999	>0.9999	>0.9999	>0.9999	>0.9999	>0.9999	>0.9999	>0.9999
GD0	>0.9999	>0.9999	0.0299	<0.0001	>0.9999	<0.0001	0.1422	<0.0001	<0.0001
GD7	0.0412	>0.9999	0.1337	<0.0001	>0.9999	0.0006	0.0200	<0.0001	<0.0001
GD14	<0.0001	>0.9999	0.0023	<0.0001	0.3043	0.0266	<0.0001	<0.0001	<0.0001
GD18	<0.0001	>0.9999	<0.0001	<0.0001	<0.0001	0.8514	<0.0001	<0.0001	<0.0001
PN8	>0.9999	NA	>0.9999	<0.0001	NA	NA	0.3711	<0.0001	<0.0001
PN15	>0.9999	NA	0.2116	<0.0001	NA	NA	0.2168	<0.0001	<0.0001

Values shown in bold indicate statistical significance. NA, not applicable.

30 and 60 min compared to LF controls (Fig. 3A and Table 3).

GDM dams showed significantly lower insulin levels compared to LF dams after 10 and 30 min (Fig. 3B and Table 3) and reduced insulin response over the first 30 min compared to HF dams (Fig. 3B and E). PDM dams exhibited more severe impairment in insulin responses (Fig. 3B and F) while insulin levels in LFSTZ dams were only significantly reduced after 10 min compared to LF dams (Fig. 3B and Table 3). Total insulin responses were modestly increased in HF compared to LF dams (Fig. 3F).

OGTTs performed in non-pregnant dams revealed significant impairments in glucose tolerance in non-pregnant HFSTZ-treated dams compared to LF/HF groups (Fig. 3G). Pregnancy resulted in significant further impairment of glucose tolerance (Fig. 3G) and higher insulin responses (Fig. 3H) in HF dams.

HF feeding does not increase BW or adiposity in GDM or PDM dams

Although HF feeding increased pre-gestational weight gain (Table 4), GD0 BWs of GDM and HF were similar to those of LF dams, while PDM dams showed significantly

higher BW (Tables 4 and 5). Gestational weight gain (GWG, Δ GD18 – GD0) was reduced in GDM, PDM, and HF compared to LF dams (Table 4) and BW throughout gestation and lactation was similar between groups (data not shown). Gonadal and perirenal adipose tissue weights were similar between groups at GD18 and reduced in GDM compared to HF, but not LF dams at PN15 (Table 4). Plasma leptin levels were not different in GDM and PDM compared to controls at both GD18 and PN15, but leptin levels were increased in HF compared to LF dams at GD18 (Table 4).

Persistent reductions of pancreatic β -cell area in GDM and PDM dams

As expected, treatment with STZ resulted in changed islet morphology (Fig. 4A). Immunofluorescent staining for insulin and glucagon revealed an increased number of α -cells per islet (Fig. 4A and B) and an increased number of islets with α -cells in the core of the islet (Fig. 4C) in GDM, PDM and LFSTZ dams, indicative for islet cell remodelling due to STZ induced β -cell death. Furthermore, islet of GDM, PDM and LFSTZ dams at GD18 showed decreased insulin expression (Fig. 4A). β -Cell area was reduced by 68% and 75% in GDM

Table 4. Overview of HF-induced weight gain, adipose tissue depot size at sacrifice and plasma parameters

	LF	LFSTZ	HF	GDM	PDM	P
Pre-gestational	<i>n</i> = 16	<i>n</i> = 8	<i>n</i> = 23	<i>n</i> = 31	<i>n</i> = 16	
Diet period weight gain (g)*	2.2 ± 0.9 ^a	1.2 ± 1.2 ^a	4.4 ± 2.1 ^b	2.6 ± 1.7 ^{ac}	4.0 ± 1.4 ^{bc}	<0.0001
Weight at GD0*	21.8 ± 1.6 ^a	21.7 ± 1.4 ^a	23.7 ± 2.8 ^{ab}	22.1 ± 2.2 ^a	24.5 ± 2.2 ^b	0.001
GD18	<i>n</i> = 6	<i>n</i> = 8	<i>n</i> = 6	<i>n</i> = 8	<i>n</i> = 5	
GWG (%)*	63 ± 14 ^a	64 ± 10 ^{ac}	41 ± 13 ^b	52 ± 11 ^c	41 ± 8 ^b	<0.0001
pWAT(% of BW)	0.48 ± 0.25	0.47 ± 0.16	0.58 ± 0.19	0.39 ± 0.22	0.54 ± 0.28	0.546
gWAT (% of BW)	0.70 ± 0.14	0.80 ± 0.22	1.30 ± 0.47	0.86 ± 0.51	1.15 ± 0.21	0.028
Plasma TG (mmol/l)	0.66 ± 0.21	0.78 ± 0.13	0.49 ± 0.17	0.65 ± 0.20	0.83 ± 0.54	0.060
Plasma NEFA (mmol/l)	0.47 ± 0.18	0.30 ± 0.11	0.45 ± 0.09	0.40 ± 0.06	0.47 ± 0.10	0.069
Plasma leptin (ng/ml)	29 ± 14 ^a	91 ± 54 ^{ab}	135 ± 67 ^b	63 ± 68 ^{ab}	61 ± 27 ^{ab}	0.025
PN15	<i>n</i> = 10	NA	<i>n</i> = 9	<i>n</i> = 12	<i>n</i> = 4	
LWG (%)	18 ± 7		23 ± 9	15 ± 5	17 ± 11	0.090
pWAT (% of BW)	0.59 ± 0.27		1.04 ± 0.55	0.49 ± 0.30	0.77 ± 0.82	0.052
gWAT (% of BW)	0.86 ± 0.40 ^{ab}		1.82 ± 0.82 ^b	0.84 ± 0.47 ^a	1.02 ± 0.83 ^{ab}	0.024
Plasma TG (mmol/l)	0.32 ± 0.17		0.48 ± 0.22	0.50 ± 0.28	0.46 ± 0.18	0.397
Plasma NEFA (mmol/l)	0.25 ± 0.09		0.38 ± 0.11	0.31 ± 0.12	0.26 ± 0.15	0.096
Plasma Leptin (ng/ml)	2.9 ± 1.3		5.4 ± 3.6	3.8 ± 2.5	8.5 ± 5.8	0.036

Data are presented as means ± SD. Statistical analysis was performed using one way ANOVA followed by Tukey's multiple comparison test in cases of normally distributed parameters (indicated by *) and using the Kruskal–Wallis test followed by Dunn's multiple comparison test in cases of non-normally distributed parameters or when power was too low to assess normality. Overall *P*-values are given in the last column. Groups that do not share common letter superscripts are significantly different (*P* < 0.05) upon *post hoc* testing. Values in bold indicate statistical significance. GD, gestational day; GDM, gestational diabetes mellitus; gWAT, gonadal white adipose tissue; GWG, gestational weight gain; HF, high fat diet; LF, Low fat diet; LWG, lactation weight gain; NA, not applicable; NEFA, non-esterified fatty acids; PDM, pre-gestational diabetes mellitus; PN, postnatal day; pWAT, perirenal white adipose tissue; TG, triglycerides.

Table 5. Correlations between random glucose at GD0 and GD18 and other parameters

Parameter	GDM			HFSTZ			LFSTZ		
	<i>r</i>	<i>r</i> ²	<i>P</i>	<i>r</i>	<i>r</i> ²	<i>P</i>	<i>r</i>	<i>r</i> ²	<i>P</i>
GD0 glucose		<i>n</i> = 31			<i>n</i> = 47			<i>n</i> = 8	
Weight gain during HF period	0.23	0.05	0.222	0.55	0.3	<0.0001	-0.03	0.00	0.934
Body weight at STZ injection	0.30	0.09	0.098	0.60	0.36	<0.0001	0.85	0.73	0.007
Gestational weight gain (%)	-0.45	0.20	0.012	-0.50	0.25	0.0004	0.29	0.08	0.489
GD18 glucose		<i>n</i> = 8			<i>n</i> = 13			<i>n</i> = 8	
Pancreatic β-cell area	-0.21	0.04	0.659	-0.39	0.16	0.201	-0.84	0.71	0.009
GD18 litter size	-0.08*		0.866	-0.08*		0.800	-0.06	0.00	0.891
PN2 litter size [†]	-0.37	0.14	0.084	-0.32	0.10	0.067			
GD18 no. of resorptions	0.39*		0.369	0.58*		0.038	0.73*		0.071
Liver weight	0.47	0.22	0.244	0.74	0.55	0.004	0.70	0.49	0.054
Plasma ALT	0.88	0.77	0.004	0.86	0.74	0.0001	0.69	0.48	0.056
NAFLD activity score	0.78*		0.030	0.90*		<0.0001	-0.08*		0.999
Hepatic mitotic figures	0.70	0.49	0.054	0.54	0.30	0.055	0.43	0.19	0.284
Hepatic apoptotic figures	0.85	0.73	0.007	0.77	0.60	0.002	0.06*		0.999
Hepatic triglycerides	0.03	0.00	0.952	-0.09	0.01	0.771	0.18	0.03	0.675

[†] GDM (*n* = 23), HFSTZ (*n* = 34), LFSTZ (*n* = 8). Correlation analysis was performed using Pearson's coefficient in cases of normally distributed parameters and using Spearman's coefficient in cases of non-normally distributed parameters (indicated by *). Values in bold indicate statistical significance. ALT, alanine aminotransferase; GD, gestational day; HF, high fat diet; LF, low fat diet; NAFLD, non-alcoholic fatty liver disease; PN, postnatal day; STZ, streptozotocin.

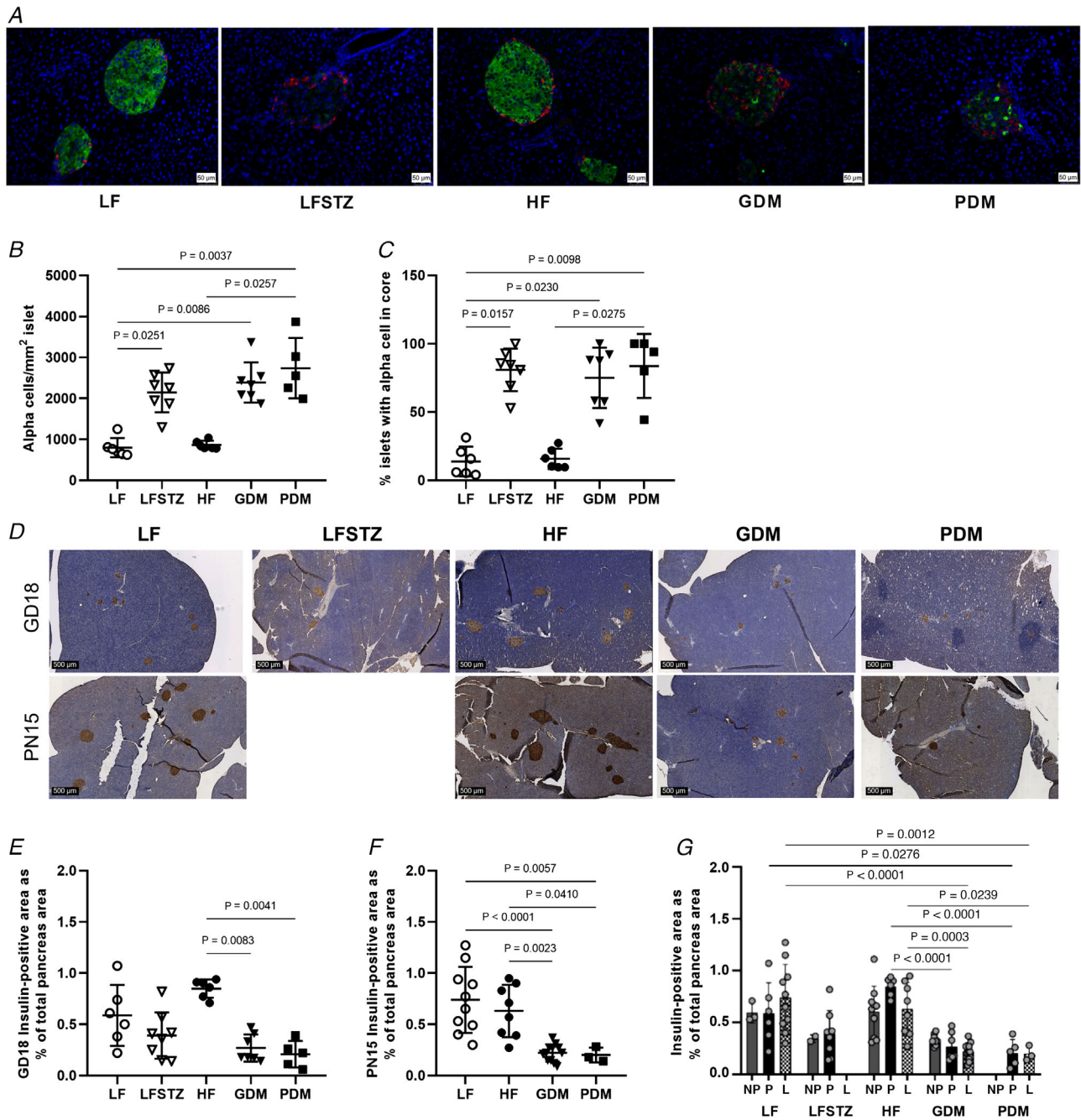


Figure 4. HFSTZ treatment results in a lasting reduction of pancreatic beta-cell area

A, representative images of immunofluorescence staining of insulin/glucagon. B, quantification of number of α -cells per mm² islet. C, percentage of islets with α -cells in the core. D, representative images of immunohistochemical insulin staining. E, semi-quantification of insulin-positive pancreas area at GD18, using eight pancreatic sections per dam. F, semi-quantification of insulin-positive pancreas area at PN15, using eight pancreatic sections per dam. G, semi-quantification of insulin-positive pancreas area in non-pregnant dams, at GD18, and at PN15, using 8 pancreatic sections per dam. Kruskal–Wallis test followed by Dunn’s multiple comparison test (A and B) and mixed model analysis followed by Bonferroni’s correction (C) were used. GD, gestational day; GDM, gestational diabetes mellitus; HF, high fat diet; L, lactation; LF, low fat diet; LFSTZ, low fat + streptozotocin; NP, non-pregnant; P, pregnant; PDM, pregestational diabetes mellitus; PN, postnatal day.

and PDM dams (GDM: $0.27 \pm 0.13\%$, PDM: $0.21\% \pm 0.13\%$), respectively, compared to HF ($0.84 \pm 0.09\%$), but not LF dams ($0.59 \pm 0.30\%$) at GD18. (Fig. 4D and E). No significant reduction in β -cell area was observed in LFSTZ compared to LF dams (0.39 ± 0.23 vs. 0.59 ± 0.30 , $P > 0.999$), yet β -cell area in LFSTZ dams correlated with GD18 RBG values (Table 5). At PN15, β -cell area in GDM and PDM dams was significantly reduced (GDM: $0.22 \pm 0.08\%$, PDM: $0.20 \pm 0.07\%$) compared to HF and LF dams (HF: $0.63 \pm 0.26\%$, LF: $0.74 \pm 0.32\%$, Fig. 4F). Compared to non-pregnant dams, no increase in pancreatic β -cell area was observed in any of the groups by GD18 ($P = 0.397$, Fig. 4G). Together, this indicates that the HFSTZ treatment decreases β -cell area, which persists during pregnancy and lactation.

GDM dams develop hyperglycaemia over the course of gestation and recover postpartum

GDM dams displayed elevated RBG concentrations compared to LF (GD0, GD14–18, Fig. 5A and Table 3) and HF (GD7–18, Fig. 5A and Table 3) that increased over gestation. Postnatally, RBG dropped to levels similar to pre-gestation and LF/HF levels (PN8/PN15, Fig. 5A and Table 3), with only 25% of GDM dams remaining hyperglycaemic postpartum (PN15). This transient hyperglycaemia was not observed in non-pregnant HFSTZ dams, confirming the gestation specificity (Fig. 5B). PDM dams displayed consistently elevated RBG levels throughout gestation and lactation (Fig. 5A and Table 3). Remarkably, LFSTZ dams developed severe hyperglycaemia throughout pregnancy, and similar progression

of hyperglycaemia was observed in non-pregnant LFSTZ animals (Fig. 5A and B, and Table 3). HF dams did not develop hyperglycaemia, regardless of pregnancy (Fig. 5A and B, and Table 3). Random insulin concentrations were similar between groups (Fig. 5C). Altogether, this indicates that HFSTZ-induced GDM indeed develops over gestation and is transient, while PDM, LFSTZ and HF dams do not exhibit this gestation-specific hyperglycaemic phenotype.

Impaired EGP suppression in GDM and PDM is dissociated from insulin sensitivity

Inclusion of stably labelled glucose during the OGTT at GD15 allowed for detailed assessment of glucose kinetics. The suppression of EGP during the first hour of the OGTT (t_{10} – t_{60}) was significantly reduced in GDM and PDM dams compared to HF, but not LF dams (Fig. 6A and B). In LFSTZ dams, EGP suppression was also reduced compared to LF dams (Fig. 6A and B), while first hour liver insulin sensitivity (IS-L) was similar between groups (Fig. 6C). The glucose clearance rate constant (k_2) was reduced in GDM and PDM dams compared to LF/HF groups (Fig. 6D), while peripheral insulin sensitivity (IS-P) remained unaffected (Fig. 6E). Combined, these results indicate that differences in OGTT first hour EGP and k_2 in GDM/PDM dams are due to impaired insulin secretion rather than reduced insulin sensitivity.

PDM compromises pregnancy outcomes

Pregnancy rates were similar between groups ($P = 0.887$, Table 1). GDM, LFSTZ and HF did not affect litter size at

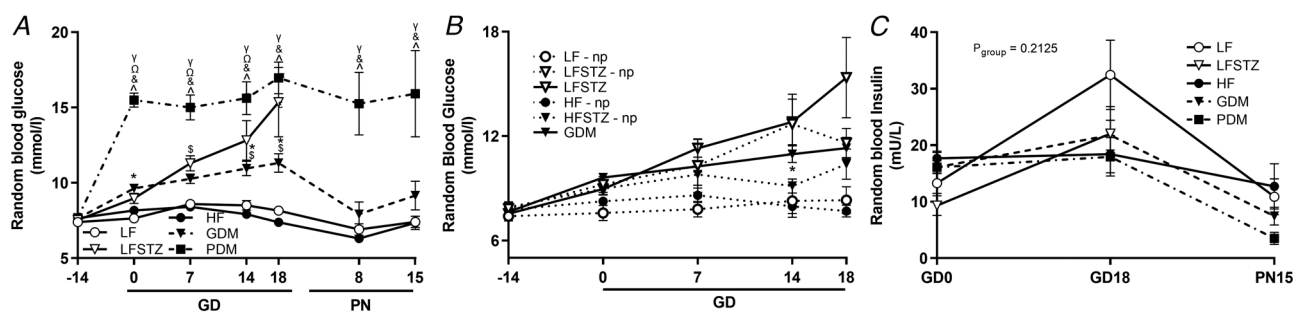


Figure 5. Pregnancy is fundamental to development of overt hyperglycaemia in GDM dams

A, unfasted RBG concentrations between the moment prior to STZ injections (GD – 14) and PN15. B, random blood glucose comparison of pregnant and non-pregnant LFSTZ and GDM animals. $*P = 0.0311$. C, unfasted random insulin concentrations throughout pregnancy and lactation. Data are displayed as means \pm SEM for readability. A and C: gestational data: $n = 16$ (LF), 8 (LFSTZ), 22 (HF), 31 (GDM), 16 (PDM). Lactation data (PN8, PN15): $n = 10$ (LF), 9 (HF), 15 (GDM), 4 (PDM), the other animals were either terminated at GD18 or switched to a LFD upon delivery for another study. B: $n = 6$ (LF-np), 10 (HF-np), 6 (LFSTZ-np), 8 (LFSTZ), 16 (HFSTZ-np), 31 (GDM). A–C: mixed model analysis followed by Bonferroni's multiple comparison test was performed. A: * GDM vs. LF, § GDM vs. HF, ¶ PDM vs. LF, $^{\&}$ PDM vs. HF, $^{\gamma}$ PDM vs. GDM, $^{\epsilon}$ LFSTZ vs. GDM, $^{\Omega}$ LFSTZ vs. PDM, $^{\alpha}$ LFSTZ vs. LF, $^{\#}$ HF vs. LF. GD, gestational day; GDM, gestational diabetes mellitus; HF, high fat diet; HFSTZ, high fat + streptozotocin; L, lactation; LF, low fat diet; LFSTZ, low fat + streptozotocin; NP, non-pregnant; P, pregnant; PDM, pregestational diabetes mellitus; PN, postnatal day.

GD18 or PN15 (Fig. 7A and C), number of resorptions at GD18 (Fig. 7B) or percentage of lost litters compared to LF ($P = 0.751$, Table 1). In contrast, PDM was associated with reduced litter size compared to GDM and HF dams (4.4 ± 1.6 vs. 6.3 ± 1.7 and 6.2 ± 1.6 pups/litter, Fig. 7C) and more resorptions than LFSTZ (2.8 ± 1.3 vs. 0.6 ± 0.5 resorptions/litter, Fig. 7B). Interestingly, the number of resorptions in GDM/PDM dams was correlated to GD18 RBG (Table 5). Additionally, litter size at PN2 was negatively correlated to GD0 RBG in GDM ($P = 0.045$, $r = -0.42$) and GDM/PDM combined ($P = 0.0006$, $r = -0.56$).

Increase in liver disease markers in PDM dams at GD18 and GDM dams at PN15

At GD18 and PN15, liver weight as a percentage of body weight was increased in GDM compared to HF, but not

LF dams (Fig. 8A). Histopathological analysis showed increased NAFLD activity scores (NAS) in livers from PDM dams at GD18, and by PN15 also in GDM, compared to HF but not LF dams (Fig. 8B and I). The increase in NAS was mostly driven by increased steatosis grade (data not shown). We found an increase in apoptotic figures and mitotic figures in PDM livers at GD18 and in GDM compared to LF and HF at PN15 (Fig. 8C and D). Plasma ALT levels at GD18 were increased in PDM compared to HF dams (Fig. 8E). Lactation was associated with a robust increase in plasma ALT levels, comparable between groups (Fig. 8E).

In GDM dams, NAS, number of apoptotic figures and plasma ALT levels positively correlated with GD18 RBG (Table 4). Moreover, plasma ALT levels correlated with liver weight ($P = 0.0081$, $r = 0.70$). None of the PN15 liver disease markers correlated to GD18 or PN15 RBG.

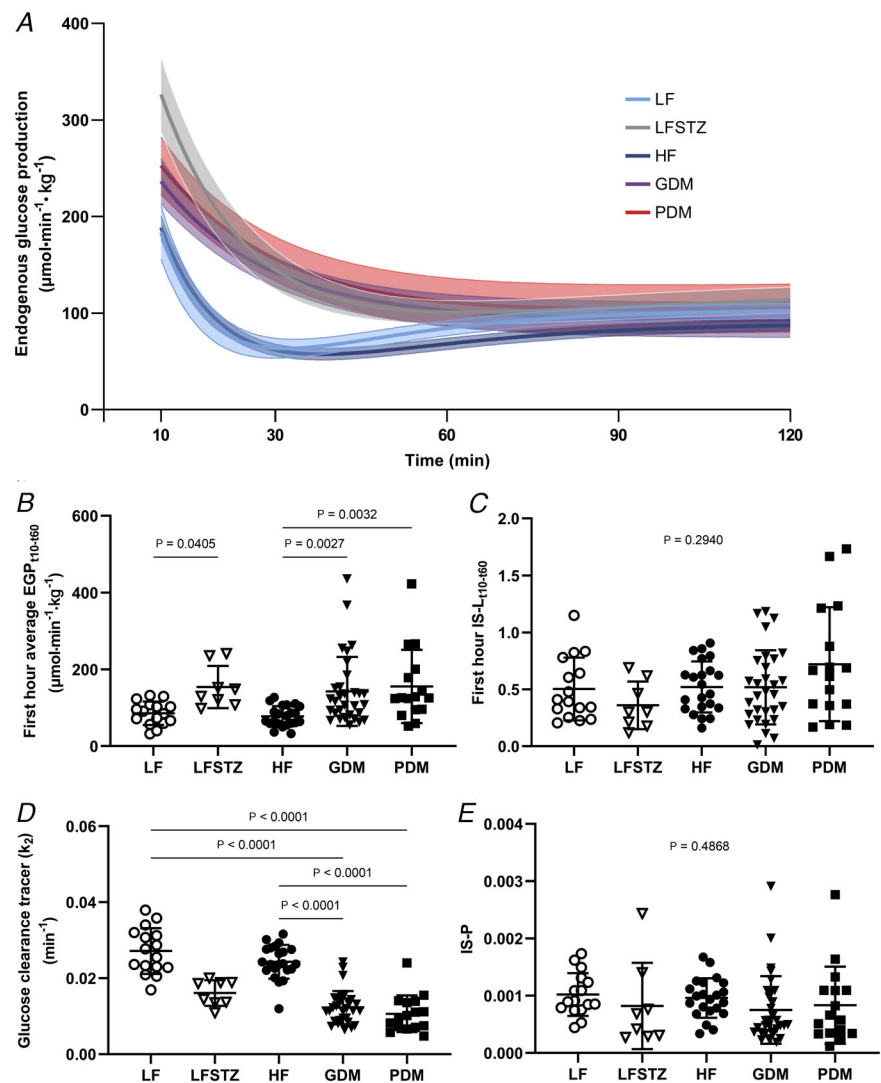


Figure 6. Lean GDM and PDM are characterized by a reduced suppression of endogenous glucose production during the first hour of an OGTT at GD15

A, endogenous glucose production during the OGTT expressed as means \pm SEM. B, average EGP from t_{10} to t_{60} calculated using $\text{AUC}_{t_{10}-t_{60}}/50$. C, IS-L as $1000 \times (\text{EGP}_{t_{10}-t_{60}} \times \text{Insulin}_{t_{10}-t_{60}})^{-1}$. D, glucose elimination rate constant (k_e). E, IS-P, calculated as $k_e(\text{labelled}) / [\text{Insulin}]_{\text{average}}$. Data are displayed as means \pm SD and a Kruskal–Wallis test followed by Dunn’s multiple comparison test was used (B–E). A–E: $n = 16$ (LF), 22 (HF), 8 (LFSTZ), 31 (GDM), 16 (PDM). AUC, area under the curve; EGP, endogenous glucose production; GD, gestational day; GDM, gestational diabetes mellitus; HF, high fat diet; IS-L, insulin sensitivity of the liver; IS-P, insulin sensitivity of the peripheral organs, including the placenta; LF, low fat diet; LFSTZ, low fat + streptozotocin; PDM, pregestational diabetes mellitus; PN, postnatal day.

Table 6. Effects of postnatal switch to LF on liver triglycerides, cholesterol esters and NAS

	LF <i>n</i> = 10	HF <i>n</i> = 9	GDM <i>n</i> = 12	GDM-LF <i>n</i> = 11	PDM <i>n</i> = 4	PDM-LF <i>n</i> = 7	<i>P</i>
TG	76 ± 25 ^{ab}	56 ± 24 ^{ac}	102 ± 25 ^b	53 ± 24 ^{ac}	108 ± 33 ^b	26 ± 23 ^c	<0.0001
Ch. esters	9.4 ± 2.5 ^a	3.0 ± 0.9 ^b	3.0 ± 1.2 ^b	6.8 ± 2.4 ^{ab}	5.1 ± 2.4 ^{ab}	3.6 ± 3.0 ^b	<0.0001
NAS	2.5 ± 1.6 ^{ab}	1.2 ± 1.0 ^a	4.3 ± 1.5 ^b	2.0 ± 1.0 ^{ab}	4.3 ± 0.6 ^{ab}	NA	0.0011

For the PDM-LF, only a selection of samples (*n* = 2) was analysed histologically, so these data were not added. The Kruskal–Wallis test followed by Dunn's multiple comparison test was used. Ch., cholesterol; GDM, gestational diabetes mellitus; HF, high fat; LF, low fat; NAS, NAFLD activity score; PDM, pregestational diabetes mellitus; TG, Triglyceride.

GDM and PDM promote hepatic lipid accumulation postpartum

Hepatic glycogen and lipid levels were largely comparable between groups at GD18 (Fig. 8F–H), while liver TG levels were increased in GDM and PDM compared to HF by PN15 (102 ± 25 and 108 ± 33 vs. 56 ± 24 nmol/mg liver, Fig. 8F). Hepatic cholesterol ester levels were elevated in LF animals at PN15 compared to GD18, and significantly lower in GDM and HF compared to LF animals (3.9 ± 1.2 and 3.0 ± 0.9 vs. 9.4 ± 2.5 nmol/mg liver, Fig. 8H). Plasma TGs and non-esterified fatty acid levels were comparable between groups at GD18 and PN15 (Table 4). The postnatal effects of GDM/PDM on liver TG, cholesterol esters and NAS were HF-dependent, as they were not observed in dams that were switched to a LF at PN2 (Table 6). Overall, these findings indicate that lean, HFSTZ-induced GDM/PDM predisposes to postpartum NAFLD development.

Discussion

In the current study we assessed the impact of HIP on maternal glucose homeostasis, adiposity, liver disease susceptibility and perinatal outcomes during pregnancy and lactation. HFSTZ treatment in mice either induced

mild hyperglycaemia, which developed during pregnancy and in most cases returned to normoglycaemia postpartum (GDM), or more severe hyperglycaemia, which already presented prior to mating (PDM). Both GDM and PDM were characterized by glucose intolerance, inadequate insulin response and reduced suppression of EGP upon an oral glucose load. These alterations were not paralleled by changes in insulin sensitivity and adiposity. Moreover, PDM, but not GDM, impacted pregnancy outcomes, i.e. higher resorptions and smaller litter size. Finally, we showed that HIP was associated with early liver disease markers in late pregnancy and lactation, as evidenced by increased NAS, hepatic TGs and plasma ALT levels, which positively correlated to the severity of hyperglycaemia.

In published preclinical models, HF is frequently used to induce obesity and subsequent insulin resistance, while STZ is used to impair insulin secretion (Pasek & Gannon, 2013). We showed that an approach combining short-term HF and STZ could provoke a clear GDM phenotype (Li et al., 2020). Our HF regimen did not, however, induce increased adiposity nor insulin resistance. STZ treatment strongly reduced pancreatic β -cell area in GDM/PDM dams and OGTT insulin responses were attenuated. Additionally, islet cell remodelling due to β -cell death was observed. This suggests that the lean GDM phenotype

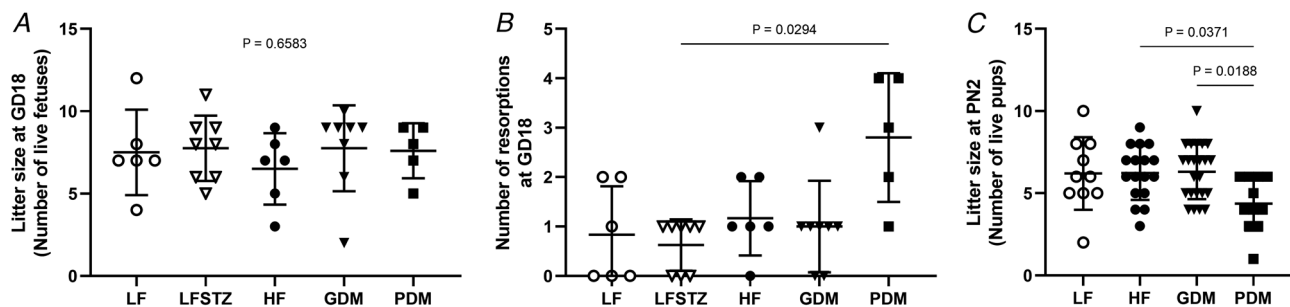


Figure 7. Litter size and resorptions were negatively affected by PDM, but not GDM

A, number of live fetuses per litter on GD18. B, number of resorptions (haemorrhagic sites) per litter on GD18. C, number of live pups per litter on PN2. Data are displayed as means ± SD. A Kruskal–Wallis test followed by Dunn's multiple comparison test (A and B) or one-way ANOVA followed by Tukey's multiple comparison test (C) was used. GD, gestational day; GDM, gestational diabetes mellitus; HF, high fat diet; LF, low fat diet; LFSTZ, low fat + streptozotocin; PDM, pregestational diabetes mellitus; PN, postnatal day.

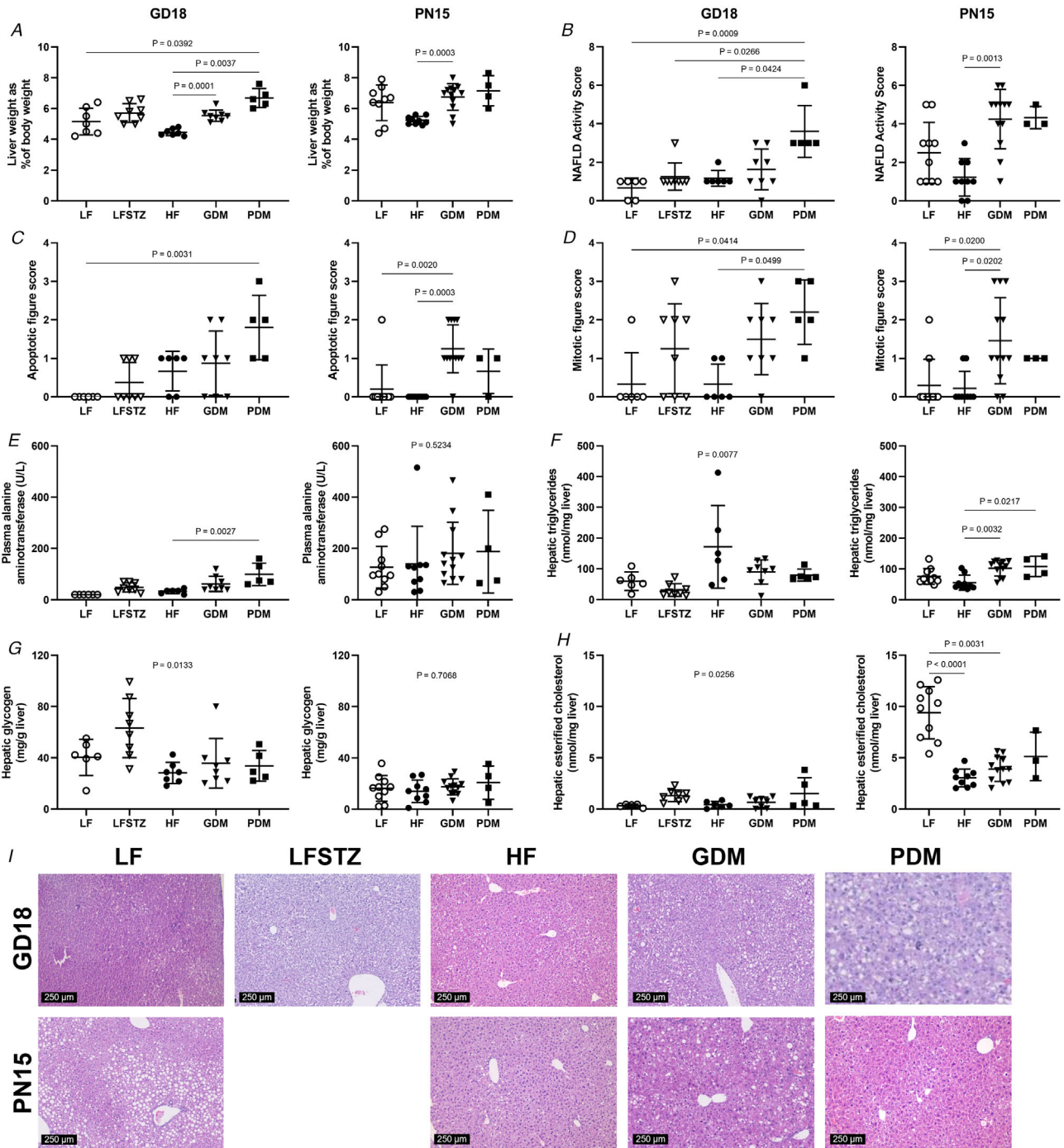


Figure 8. HFSTZ-induced lean GDM and PDM induce early signs of postpartum NAFLD development
 GD18, left panel; PN15, right panels. **A**, liver weight as a percentage of body weight. **B**, NAFLD activity score (NAS) derived from pathological assessment of liver H&E slides. Score is composed of lobular inflammation, steatosis grade and ballooning. **C**, apoptotic figure score derived from pathological assessment of liver H&E slides. **D**, mitotic figure score derived from pathological assessment of liver H&E slides. **E**, plasma alanine aminotransferase concentration (ALT). **F**, hepatic triglyceride content. **G**, hepatic glycogen content. **H**, hepatic esterified cholesterol content. **I**, representative liver H&E images. Data are displayed as means ± SD and the Kruskal–Wallis test followed by Dunn’s multiple comparison test was used (A–H). For **F**, **G** and **H**, the GD18 Kruskal–Wallis test was significant, but no statistically significant differences were detected by Dunn’s multiple comparison test. GD18: *n* = 6 (LF), 6 (HF), 8 (LFSTZ), 8 (GDM), 5 (PDM). PN15: *n* = 10 (LF), 9 (HF), 12 (GDM), 4 (PDM). GD, gestational day; GDM, gestational diabetes mellitus; H&E, haematoxylin and eosin; HF, high fat diet; LF, low fat diet; LFSTZ, low fat + streptozotocin; NAFLD, non-alcoholic fatty liver disease; PDM, pregestational diabetes mellitus; PN, postnatal day.

induced by HFSTZ treatment and subsequent pregnancy is predominantly driven by STZ-induced impairment in pancreatic insulin release. Interestingly, PDM dams showed a significantly larger impairment in glucose tolerance and insulin responses yet displayed a similar reduction in pancreatic β -cell area as GDM dams, with unaltered insulin sensitivity. However, detection of subtle differences in β -cell area or insulin sensitivity between GDM/PDM dams may require larger sample sizes. Also, while glucose levels and β -cell area were correlated in LFSTZ dams, this was not observed in GDM/PDM dams. The difference in glucose tolerance between GDM and PDM dams therefore warrants further research.

The lean, insulin sensitive GDM in this model mimics the phenotype of insulin secretion-driven GDM in humans (Benhalima et al., 2019; Liu et al., 2018; Pasek & Gannon, 2013; Powe et al., 2016; Wang et al., 2020). This GDM subtype mostly occurs in non-obese, insulin sensitive women (Powe et al., 2016) and is further characterized by reduced fasting insulin and insulin response during the first 30 min of an OGTT (Benhalima et al., 2019; Cheney et al., 1985; Powe et al., 2016). Although our GDM mice showed unaltered fasting insulin levels, their initial insulin responses were indeed severely impaired. Together, these findings indicate that this pre-clinical model adequately reflects characteristics of GDM and PDM in non-obese women.

The absence of HF-induced adiposity and insulin resistance was not expected. Although our HF groups were heavier at GD0, GWG was lower, resulting in similar BWs between groups throughout gestation. Previous studies also reported lower GWG in mice on obesogenic diets (Liang et al., 2010; Samuelsson et al., 2008). In human pregnancy, GWG is also lower in overweight/obese women (Siega-Riz et al., 2020), but excess GWG is also a risk factor for GDM (McDowell et al., 2019). Although HF is well-established to induce adiposity and insulin resistance in BL/6N mice, females are relatively resistant to these complications (Hwang et al., 2010; Ingvorsen et al., 2017; Taconic Biosciences, 2022). Notably, short term high fat/high sugar feeding in females can actually impair pregnancy-induced increase in β -cell area and insulin response (Pennington et al., 2017). The absence of insulin resistance in HF-treated groups may question the contribution of HF in the experimental approach. Yet, the hyperglycaemia observed in LFSTZ-treated dams was not mild or pregnancy-specific in this study, nor in previous work (Li et al., 2020). Although the exact mechanisms remain unclear, our data indicate that the HF regimen is essential for induction of a translational, gestation-specific GDM phenotype in STZ-treated mice.

The use of stably labelled glucose during the OGTT generated unique insights on glucose and insulin metabolism and allowed dissection of the EGP from the glucose elimination by peripheral tissues (van Dijk

et al., 2013; Vieira-Lara et al., 2023). We showed an impairment in first hour EGP suppression and reduced glucose clearance in GDM/PDM dams, while IS-P and IS-L remained unaffected. This confirms that defective insulin secretion, rather than reduced insulin sensitivity, drives the GDM/PDM phenotypes observed. Limitations of the modelling approach are: (1) calculated EGP depends on rate constants, which were assumed to be constant over the entire glucose curve rather than specific for each time point as our OGTT data do not allow fitting of a more complex model (Cobelli et al., 2014; Vieira-Lara et al., 2023); (2) the approach does not allow us to dissect glucose- and insulin-mediated effects, and thus the calculated insulin sensitivity indices cover both.

Women with former (lean) GDM are at risk for development of metabolic complications such as type 2 diabetes and NAFLD postpartum (Ajmera et al., 2016; Chen et al., 2021; Forbes et al., 2011). In agreement with these human data, we observed that a subgroup of GDM dams did not recover from gestational hyperglycaemia by PN15 and may develop overt diabetes over time. Interestingly, signs of postpartum NAFLD development, such as an increased NAS and elevated plasma ALT levels, were observed by PN15 in GDM/PDM dams, but already at GD18 in PDM dams. This increase in NAFLD markers is likely related to the higher GD18/PN15 hepatic TG contents in GDM and PDM dams. Moreover, the number of hepatic apoptotic figures, which are associated with NAFLD progression (Kanda et al., 2018), was increased. Although we did not investigate the molecular mechanisms underlying this NAFLD in detail, we speculate that increased inflammation and subsequent oxidative stress may be important drivers (Donnelly et al., 2019; Minooee et al., 2017). These findings suggests that our preclinical model allows the study of postpartum NAFLD development after diabetic pregnancy. Although clinical studies have focused on the association between GDM and NAFLD (Kubihal et al., 2021; Lavrentaki et al., 2019), assessments were usually performed several years postpartum. Our results show increases in NAFLD markers already during lactation, illustrating the need for early and more intensive NAFLD monitoring in women with former HIP. Obviously, these results also underscore the need for earlier detection and treatment of gestational hyperglycaemia to mitigate adverse consequences like NAFLD.

Besides inducing metabolic risks, HIP is associated with adverse pregnancy outcomes. We found that PDM, but not GDM, increased the number of resorptions and resulted in smaller PN2 litter sizes, and associated with pre-pregnancy blood glucose levels. Similarly, a mouse study using short-term high fat high/high sugar feeding reported a reduced litter survival throughout lactation in the high fat/high sugar-fed group (Lean et al., 2022). Consistent with these findings, higher rates of stillbirths

were reported in human PDM and GDM (Dudley, 2007; Mackin et al., 2019; Stacey et al., 2019), and associated with HbA1c (Rackham et al., 2009). This emphasizes the need for earlier detection of HIP, better monitoring and clinical care to improve pregnancy outcomes.

In contrast to previous animal models based on STZ and/or HF (Li et al., 2020; Pasek & Gannon, 2013), the current preclinical approach induces a unique (mostly) transient hyperglycaemia that more closely mimics the human situation. The high reproducibility of the model, which is often challenging in preclinical research (Kafkafi et al., 2018), is another strength. The prevalence of HIP subtypes induced by HFSTZ in this study was comparable to that observed previously (Li et al., 2020) as well as among different sub-cohorts within the current study. However, the HFSTZ treatment resulted in limited dams with the PDM phenotype leaving the PDM group underpowered. Given the absence of insulin resistance, our model only represents lean, insulin sensitive GDM, and its translational value remains to be further established. While the overt hyperglycaemia in our model is transient and pregnancy-dependent, we did observe changes in glucose tolerance in our non-pregnant HFSTZ-treated dams, which may limit translatability to human GDM. The use of STZ represents another limitation, as this agent dramatically affects pancreatic function and may already have impacted glucose and insulin metabolism prior to mating, as suggested by our observations in non-pregnant controls (Fig. 5B). Although no clear diagnostic cutoff values for murine GDM exist (Capobianco et al., 2016; Li et al., 2020; Szlapinski et al., 2019), the approach used clearly discriminated between GDM and PDM (Li et al., 2020). Importantly, the induction of pre-gestational and gestational hyperglycaemic phenotypes allowed us to study the relationship between the time of onset and severity of hyperglycaemia on different outcomes during late pregnancy and lactation.

Altogether, we showed that our preclinical model provides an adequate reflection of GDM and PDM in non-obese women, providing added value for pre-clinical HIP research and translational strength. The links between hyperglycaemic severity and different outcomes offers a starting point to test possible interventions to ameliorate the adverse effects of GDM/PDM on pregnancy and long-term health outcomes in mother and offspring.

References

- Ajmera, V. H., Gunderson, E. P., VanWagner, L. B., Lewis, C. E., Carr, J. J., & Terrault, N. A. (2016). Gestational diabetes mellitus is strongly associated with non-alcoholic fatty liver disease. *American Journal of Gastroenterology*, **111**(5), 658–664.
- Benhalima, K., van Crombrugge, P., Moyson, C., Verhaeghe, J., Vandeginste, S., Verlaenen, H., Vercammen, C., Maes, T., Dufraimont, E., de Block, C., Jacquemyn, Y., Mekahli, F., de Clippel, K., van den Bruel, A., Loccufier, A., Laenen, A., Minschart, C., Devlieger, R., & Mathieu, C. (2019). Characteristics and pregnancy outcomes across gestational diabetes mellitus subtypes based on insulin resistance. *Diabetologia*, **62**(11), 2118–2128.
- Bergmeyer. (1974). *Methods of Enzymatic Analysis*. New York Academic Press.
- Capobianco, E., Fornes, D., Linenberg, I., Powell, T. L., Jansson, T., & Jawerbaum, A. (2016). A novel rat model of gestational diabetes induced by intrauterine programming is associated with alterations in placental signaling and fetal overgrowth. *Molecular and Cellular Endocrinology*, **422**, 221–232.
- Catalano, P. M. (2014). Trying to understand gestational diabetes. *Diabetic Medicine*, **31**(3), 273–281.
- Chen, L. W., Soh, S. E., Tint, M. T., Loy, S. L., Yap, F., Tan, K. H., Lee, Y. S., Shek, L. P. C., Godfrey, K. M., Gluckman, P. D., Eriksson, J. G., Chong, Y. S., & Chan, S. Y. (2021). Combined analysis of gestational diabetes and maternal weight status from pre-pregnancy through post-delivery in future development of type 2 diabetes. *Scientific Reports*, **11**(1), 5021.
- Cheney, C., Shragg, P., & Holingsworth, D. (1985). Demonstration of heterogeneity in gestational diabetes by a 400-kcal breakfast meal tolerance test. *Obstetrics and Gynecology*, **65**(1), 17–23.
- Cobelli, C., Man, C. D., Toffolo, G., Basu, R., Vella, A., & Rizza, R. (2014). The oral minimal model method. *Diabetes*, **63**(4), 1203–1213.
- Dommerholt, M. B., Blankestijn, M., Vieira-Lara, M. A., van Dijk, T. H., Wolters, H., Koster, M. H., Gerding, A., van Os, R. P., Bloks, V. W., Bakker, B. M., Kruit, J. K., & Jonker, J. W. (2020). Short-term protein restriction at advanced age stimulates FGF21 signalling, energy expenditure and browning of white adipose tissue. *FEBS Journal*, **288**(7), 2257–2277.
- Donnelly, S. R., Hinkle, S. N., Rawal, S., Grunnet, L. G., Chavarro, J. E., Vaag, A., Wu, J., Damm, P., Mills, J. L., Li, M., Bjerregaard, A. A., Thuesen, A. C. B., Gore-Langton, R. E., Francis, E. C., Ley, S. H., Hu, F. B., Tsai, M. Y., Olsen, S. F., & Zhang, C. (2019). Prospective study of gestational diabetes and fatty liver scores 9 to 16 years after pregnancy. *Journal of Diabetes*, **11**(11), 895–905.
- Dudley, D. J. (2007). Diabetic-associated stillbirth: Incidence, pathophysiology, and prevention. *Obstetrics and Gynecology Clinics of North America*, **34**(2), 293–307.
- Farahvar, S., Walfisch, A., & Sheiner, E. (2019). Gestational diabetes risk factors and long-term consequences for both mother and offspring: A literature review. *Expert Review of Endocrinology & Metabolism*, **14**(1), 63–74.
- Ferrara, A. (2007). Increasing prevalence of gestational diabetes mellitus: A public health perspective. *Diabetes Care*, **30**(Supplement_2), S141–S146.

- Forbes, S., Taylor-Robinson, S. D., Patel, N., Allan, P., Walker, B. R., & Johnston, D. G. (2011). Increased prevalence of non-alcoholic fatty liver disease in European women with a history of gestational diabetes. *Diabetologia*, **54**(3), 641–647.
- Hübscher, S. G. (2006). Histological assessment of non-alcoholic fatty liver disease. *Histopathology*, **49**(5), 450–465.
- Hwang, L.-L., Wang, C.-H., Li, T.-L., Chang, S.-D., Lin, L.-C., Chen, C.-P., Chen, C.-T., Liang, K.-C., Ho, I.-K., Yang, W.-S., & Chiou, L.-C. (2010). Sex differences in high-fat diet-induced obesity, metabolic alterations and learning, and synaptic plasticity deficits in mice. *Obesity*, **18**(3), 463–469.
- Ingvorsen, C., Karp, N. A., & Lelliott, C. J. (2017). The role of sex and body weight on the metabolic effects of high-fat diet in C57BL/6N mice. *Nutrition & Diabetes*, **7**, e261–e261.
- International Diabetes Federation (2019). *IDF Diabetes Atlas*. https://diabetesatlas.org/upload/resources/material/20200302_133351_IDFATLAS9e-final-web.pdf
- International Diabetes Federation (2021). *IDF Diabetes Atlas 10th edition*. <https://www.diabetesatlas.org>
- Joachim, R., Zenclussen, A. C., Polgar, B., Douglas, A. J., Fest, S., Knackstedt, M., Klapp, B. F., & Arck, P. C. (2003). The progesterone derivative dydrogesterone abrogates murine stress-triggered abortion by inducing a Th2 biased local immune response. *Steroids*, **68**(10–13), 931–940.
- Kafkafi, N., Agassi, J., Chesler, E. J., Crabbe, J. C., Crusio, W. E., Eilam, D., Gerlai, R., Golani, I., Gomez-Marin, A., Heller, R., Iraqi, F., Jaljuli, I., Karp, N. A., Morgan, H., Nicholson, G., Pfaff, D. W., Richter, S. H., Stark, P. B., Stiedl, O., ..., & Benjamini, Y. (2018). Reproducibility and replicability of rodent phenotyping in preclinical studies. *Neuroscience and Biobehavioral Reviews*, **87**, 218–232.
- Kampmann, U. (2015). Gestational diabetes: A clinical update. *World Journal of Diabetes*, **6**(8), 1065.
- Kanda, T., Matsuoka, S., Yamazaki, M., Shibata, T., Nirei, K., Takahashi, H., Kaneko, T., Fujisawa, M., Higuchi, T., Nakamura, H., Matsumoto, N., Yamagami, H., Ogawa, M., Imazu, H., Kuroda, K., & Moriyama, M. (2018). Apoptosis and non-alcoholic fatty liver diseases. *World Journal of Gastroenterology*, **24**(25), 2661.
- Kim, S. Y., England, L., Wilson, H. G., Bish, C., Satten, G. A., & Dietz, P. (2010). Percentage of gestational diabetes mellitus attributable to overweight and obesity. *American Journal of Public Health*, **100**(6), 1047–1052.
- Kleiner, D. E., Brunt, E. M., van Natta, M., Behling, C., Contos, M. J., Cummings, O. W., Ferrell, L. D., Liu, Y.-C., Torbenson, M. S., Unalp-Arida, A., Yeh, M., McCullough, A. J., & Sanyal, A. J. (2005). Design and validation of a histological scoring system for nonalcoholic fatty liver disease. *Hepatology*, **41**(6), 1313–1321.
- Kubihal, S., Gupta, Y., Shalimar, K. D., Goyal, A., Kalaivani, M., Goyal, A., Kedia, S., Kachhawa, G., Ambekar, S., Bhatia, D., Garg, V., Gupta, N., & Tandon, N. (2021). Prevalence of non-alcoholic fatty liver disease and factors associated with it in Indian women with a history of gestational diabetes mellitus. *Journal of Diabetes Investigation*, **12**(5), 877–885.
- Lavrentaki, A., Thomas, T., Subramanian, A., Valsamakis, G., Thomas, N., Toulis, K. A., Wang, J., Daly, B., Saravanan, P., Sumilo, D., Mastorakos, G., Tahrani, A. A., & Nirantharakumar, K. (2019). Increased risk of non-alcoholic fatty liver disease in women with gestational diabetes mellitus: A population-based cohort study, systematic review and meta-analysis. *Journal of Diabetes and its Complications*, **33**(10), 463–469.
- Lean, S. C., Candia, A. A., Gulacsi, E., Lee, G. C. L., & Sferruzzi-Perri, A. N. (2022). Obesogenic diet in mice compromises maternal metabolic physiology and lactation ability leading to reductions in neonatal viability. *Acta Physiologica*, **236**(2), e13861.
- Lee, P. W., Bergner, A. E., & Edmond, J. (1991). Mass isotopomer analysis: Theoretical and practical considerations. *Biological Mass Spectrometry*, **20**(8), 451–458.
- Li, H. Y., Liu, Y. X., Harvey, L., Shafaeizadeh, S., van der Beek, E. M., & Han, W. (2020). A mouse model of gestation-specific transient hyperglycemia for translational studies. *Journal of Endocrinology*, **244**(3), 501–510.
- Liang, C., DeCourcy, K., & Prater, M. R. (2010). High-saturated-fat diet induces gestational diabetes and placental vasculopathy in C57BL/6 mice. *Metabolism*, **59**(7), 943–950.
- Lilao-Garzón, J., Valverde-Tercedor, C., Muñoz-Descalzo, S., Brito-Casillas, Y., & Wägner, A. M. (2020). In vivo and in vitro models of diabetes: A focus on pregnancy. *Advances in Experimental Medicine and Biology*, **1307**, 553–576.
- Liu, Y., Hou, W., Meng, X., Zhao, W., Pan, J., Tang, J., Huang, Y., Tao, M., & Liu, F. (2018). Heterogeneity of insulin resistance and beta cell dysfunction in gestational diabetes mellitus: A prospective cohort study of perinatal outcomes. *Journal of Translational Medicine*, **16**(1), 289.
- Mackin, S. T., Nelson, S. M., Wild, S. H., Colhoun, H. M., Wood, R., & Lindsay, R. S. (2019). Factors associated with stillbirth in women with diabetes. *Diabetologia*, **62**(10), 1938–1947.
- Martin, R. M., Patel, R., Zinovik, A., Kramer, M. S., Oken, E., Vilchuck, K., Bogdanovich, N., Sergeichick, N., Gunnarsson, R., Grufman, L., Foo, Y., & Gusina, N. (2012). Filter paper blood spot enzyme linked immunoassay for insulin and application in the evaluation of determinants of child insulin resistance. *PLoS ONE*, **7**(10), e46752.
- Matsuda, M., & DeFronzo, R. A. (1999). Insulin sensitivity indices obtained from oral glucose tolerance testing: Comparison with the euglycemic insulin clamp. *Diabetes Care*, **22**(9), 1462–1470.
- McDowell, M., Cain, M. A., & Brumley, J. (2019). Excessive gestational weight gain. *Journal of Midwifery & Womens Health*, **64**(1), 46–54.
- Minooee, S., Ramezani Tehrani, F., Rahmati, M., Mansournia, M. A., & Azizi, F. (2017). Dyslipidemia incidence and the trend of lipid parameters changes in women with history of gestational diabetes: A 15-year follow-up study. *Endocrine*, **58**(2), 228–235.
- Pasek, R. C., & Gannon, M. (2013). Advancements and challenges in generating accurate animal models of gestational diabetes mellitus. *American Journal of Physiology. Endocrinology and Metabolism*, **305**(11), E1327–E1338.

- Pennington, K. A., van der Walt, N., Pollock, K. E., Talton, O. O., & Schulz, L. C. (2017). Effects of acute exposure to a high-fat, high-sucrose diet on gestational glucose tolerance and subsequent maternal health in mice†. *Biology of Reproduction*, **96**(2), 435–445.
- Powe, C. E., Allard, C., Battista, M. C., Doyon, M., Bouchard, L., Ecker, J. L., Perron, P., Florez, J. C., Thadhani, R., & Hivert, M. F. (2016). Heterogeneous contribution of insulin sensitivity and secretion defects to gestational diabetes mellitus. *Diabetes Care*, **39**(6), 1052–1055.
- Rackham, O., Paize, F., & Weindling, A. M. (2009). Cause of death in infants of women with pregestational diabetes mellitus and the relationship with glycemic control. *Postgraduate Medicine*, **121**(4), 26–32.
- Samuelsson, A. M., Matthews, P. A., Argenton, M., Christie, M. R., McConnell, J. M., Jansen, E., Piersma, A. H., Ozanne, S. E., Twinn, D. F., Remacle, C., Rowleson, A., Poston, L., & Taylor, P. D. (2008). Diet-induced obesity in female mice leads to offspring hyperphagia, adiposity, hypertension, and insulin resistance: A novel murine model of developmental programming. *Hypertension*, **51**(2), 383–392.
- Schindelin, J., Arganda-Carreras, I., Frise, E., Kaynig, V., Longair, M., Pietzsch, T., Preibisch, S., Rueden, C., Saalfeld, S., Schmid, B., Tinevez, J. Y., White, D. J., Hartenstein, V., Eliceiri, K., Tomancak, P., & Cardona, A. (2012). Fiji: An open-source platform for biological-image analysis. *Nature Methods*, **9**(7), 676–682.
- Siega-Riz, A. M., Bodnar, L. M., Stotland, N. E., & Stang, J. (2020). The current understanding of gestational weight gain among women with obesity and the need for future research. *NAM Perspectives*, **2020**, 2020.
- Stacey, T., Tennant, P., McCowan, L., Mitchell, E., Budd, J., Li, M., Thompson, J., Martin, B., Roberts, D., & Heazell, A. (2019). Gestational diabetes and the risk of late stillbirth: A case–control study from England, UK. *BJOG*, **126**(9), 1184–1184.
- Szlapinski, S. K., King, R. T., Retta, G., Yeo, E., Strutt, B. J. &, & Hill, D. J. (2019). A mouse model of gestational glucose intolerance through exposure to a low protein diet during fetal and neonatal development. *The Journal of Physiology*, **597**(16), 4237–4250.
- Taconic Biosciences (2022). Body Weight. <https://www.taconic.com/phenotypic-data/body-weight/index.html>
- The HAPO Study Cooperative Research Group (2008). Hyperglycemia and adverse pregnancy outcomes. *New England Journal of Medicine*, **358**(19), 1991–2002.
- van Dijk, T. H., Laskewitz, A. J., Grefhorst, A., Boer, T. S., Bloks, V. W., Kuipers, F., Groen, A. K., & Reijngoud, D. J. (2013). A novel approach to monitor glucose metabolism using stable isotopically labelled glucose in longitudinal studies in mice. *Laboratory Animals*, **47**(2), 79–88.
- Vieira-Lara, M. A., Reijne, A. C., Koshian, S., Ciapaite, J., Abegaz, F., Talarovicova, A., Dijk van, T. H., Versloot, C. J., Bandsma, R. H. J., Wolters, J. C., Kuipers, F., Groen, A. K., Reijngoud, D.-J., Dijk van, G., & Bakker, B. M. (2023). Age and diet modulate the insulin-sensitizing effects of exercise: A tracer-based oral glucose tolerance test. *bioRxiv*. <https://doi.org/10.1101/2023.03.18.533083>
- Wang, N., Song, L., Sun, B., Peng, Y., Fei, S., Cui, J., Mi, Y., & Cui, W. (2020). Contribution of gestational diabetes mellitus heterogeneity and prepregnancy body mass index to large-for-gestational-age infants—A retrospective case-control study. *J Diabetes*, **13**(4), 307–317.
- Zisser, H. C., Biersmith, M. A., Jovanović, L. B., Yogeve, Y., Hod, M., & Kovatchev, B. P. (2010). Fetal risk assessment in pregnancies complicated by diabetes mellitus. *Journal of Diabetes Science and Technology*, **4**(6), 1368–1373.

Additional information

Data availability statement

The datasets generated and analysed during the current study are available from the corresponding author on reasonable request.

Competing interests

E.M.vd.B. was an employee of Danone Nutricia Research (Utrecht, the Netherlands) at the time the study was started. Currently, she is employed at Nestlé Research (Lausanne, Switzerland). The other authors declare that there are no relationships or activities that might bias, or be perceived to bias, their work.

Author contributions

A.J.C.T., E.M.vd.B. and M.H.O. conceived the topic and designed the experimental approach. All authors substantially contributed to data collection and analyses. Statistical analyses were done by A.J.C.T., K.H., J.K. and M.A.V.L. Drafting of the manuscript was done by A.J.C.T. All authors interpreted data, added sections to the manuscript involving their expertise and critically reviewed the final manuscript for intellectual content. A.J.C.T. is the guarantor of this work and, as such, had full access to all the data in the study and takes responsibility for the integrity of the data and the accuracy of the data analysis. All authors have read and approved the final version of this manuscript and agree to be accountable for all aspects of the work in ensuring that questions related to the accuracy or integrity of any part of the work are appropriately investigated and resolved. All persons designated as authors qualify for authorship, and all those who qualify for authorship are listed.

Funding

This work was supported by Danone Nutricia Research. The funder contributed to the conception of the study and the study design and reviewed the final manuscript. The funder did not contribute to the conduct of the study, sample collection, analysis of samples, interpretation of data, and did not impose any restrictions regarding the publication of the report. M.H.O. holds a Rosalind Franklin Fellowship from the University of Groningen. K.H. is co-financed by the Ministry of Economic Affairs and Climate Policy by means of the PPP-allowance made available by the Top Sector Life Sciences & Health to stimulate public-private partnerships.

Acknowledgements

The authors would like to thank T. H. van Dijk, D. J. Dijkstra, A. Soliman and Y. Yu (University Medical Centre Groningen) for

their technical assistance. The authors are grateful to L. Harvey (Danone Nutricia Research, Utrecht) for critical reading.

Keywords

endogenous glucose production, gestational diabetes mellitus, insulin secretion, non-alcoholic fatty liver disease, pre-gestational diabetes, pregnancy outcomes

Supporting information

Additional supporting information can be found online in the Supporting Information section at the end of the HTML view of the article. Supporting information files available:

Statistical Summary Document

Peer Review History

Translational perspective

In this paper, the relationship between maternal hyperglycaemia and (postpartum) maternal metabolic health and pregnancy outcomes was explored. Maternal gestational hyperglycaemia resulted in impaired pregnancy outcomes, such as litter size, and an increase in markers of non-alcoholic fatty liver disease (NAFLD) postpartum. Several of these were directly correlated to maternal glucose levels in late gestation, which stresses the importance of glycaemic monitoring and tight glycaemic control in human gestational diabetes mellitus (GDM). Furthermore, while associations between GDM and long-term risk of NAFLD development have been described before, the increased risk of short-term postpartum NAFLD development is yet to be explored. These findings signal the need for early and more rigorous NAFLD screening in postpartum GDM women. Earlier diagnosis of NAFLD would allow for better treatment and improved long-term outcomes, such as lower progression rates towards non-alcoholic steatohepatitis and prevention of subsequent cirrhosis and liver cancer.